

Identification of Image-Potential Surface States on Metals

D. Straub and F. J. Himpsel

IBM T. J. Watson Research Center, Yorktown Heights, New York 10598

(Received 19 December 1983)

Rydberg-like surface states are identified at Au(100) and Cu(100) surfaces by use of inverse photoemission with tunable photon energy. The binding energy (0.6 eV below vacuum) and width (≤ 0.3 eV full width at half maximum) of the $n = 1$ state agree well with previous calculations. Theory yields the expectation that these states represent a widespread phenomenon at surfaces.

PACS numbers: 73.20.Cw, 79.20.Kz, 79.60.Cn

Surface states in the band gaps of free-electron-like s,p bands are common to many surfaces. Predicted already in 1939 by Shockley,¹ such states have been observed in photoemission from a wide class of metal surfaces.²⁻⁶ A very special case arises when such states are located in a gap which contains the vacuum level. Then the effective potential for a surface electron can be greatly simplified into an image-charge potential combined with a repulsive barrier at the surface⁷⁻⁹ (see Fig. 1). There exists a Rydberg-type series of bound states in this potential with energies $E_n = -(1 \text{ Ry})/[16(n+a)^2]$ converging towards the vacuum energy whereby the quantum defect a ranges from $-\frac{1}{2}$ to $+\frac{1}{2}$. Echenique and Pendry⁹ calculated $a = 0.21$ in a realistic case. For finite momentum parallel to the surface (k_{\parallel}) one has to add the kinetic energy $(\hbar k_{\parallel})^2/2m$. The striking features of these image-potential surface states are their simplicity and widespread occurrence. They are expected not only for metals with s,p band gaps but also for many insulators where the conduction-band minimum lies above the vacuum level such as in many molecular solids and liquids.⁷ Applications include trapping of electrons on the surface of quantum fluids.⁷

Image-potential states are difficult to access with conventional surface-state probes such as photoemission and secondary-electron spectroscopy because the electrons are bound outside the escape cone [given by $\hbar k_{\parallel} \leq (2mE)^{1/2}$] and cannot leave the surface. Indirect evidence has been collected from the observation of resonances in the emission of elastic and inelastic electrons.¹⁰⁻¹⁴ These resonances occur just below the threshold for the emergence of new diffracted beams. They have been explained by a resonance coupling between bound image-potential states and propagating diffraction beams,^{9,10} but later on interference effects have been proposed as an alternative interpretation.^{13,14} However, interference effects can be excluded by direct observation of the lowest image-potential

state which lies below the vacuum level and which, therefore, cannot interfere with the continuum. Inverse photoemission (or bremsstrahlung spectroscopy)¹⁵ is an ideal technique for probing bound states directly by measuring their energy and momentum via the energy and momentum of an incident electron and the energy of the emitted photon. It has been recognized^{16,17} that a shoulder located just below the vacuum level (E_{vac}) in inverse photoemission spectra from Ni(100) and Cu(100) could be a candidate for an unresolved Rydberg series of image-potential states. However, this conclusion was not definitive because an energy-loss satellite could provide an equally con-

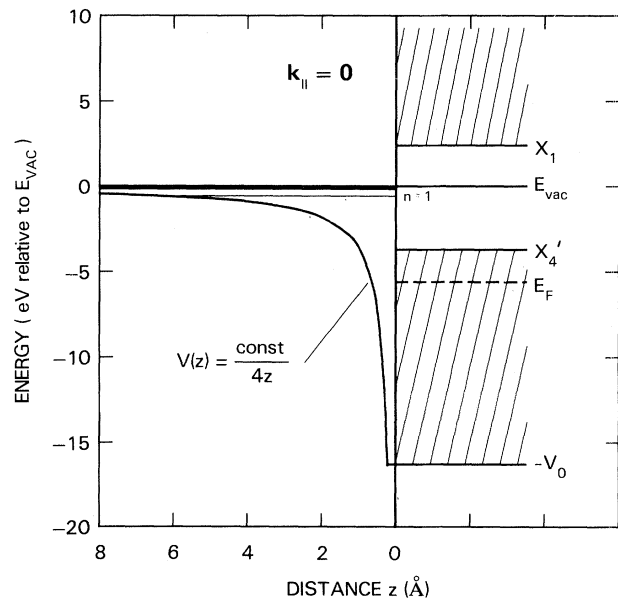


FIG. 1. Model potential diagram for image-potential surface states on Cu(100). The wave function of an electron trapped in its image potential cannot penetrate into the solid, since there is a band gap of bulk states between X_4' and X_1 .

vincing explanation.¹⁶

We are able to resolve the $n = 1$ image-potential state using a high-resolution spectrometer. The explanation as an energy-loss satellite can be ruled out because of the sharpness of the line. By tuning the photon energy $h\nu$ at fixed k^{\parallel} the two-dimensional character of the surface state is demonstrated: Three-dimensional bulk states are seen to disperse with $h\nu$ (because k^{\perp} changes) as opposed to the image-potential state which remains stationary. The energy positions and width calculated by Echenique and Pendry⁹ for the $n = 1$ state agree with our data within our measurement accuracy.

The experiment was performed with a new inverse photoemission spectrometer (see Ref. 15) which contains a fast monochromator ($f/4$ grating with simultaneous detection of all photon energies from 8 to 28 eV) and a BaO electron source in a Pierce geometry. The energy and momentum resolution was mainly limited by the thermal spread of the electrons (≈ 0.25 eV and 0.1 \AA^{-1} , respectively). For each spectrum the electron energy was kept fixed and the spectrum of bremsstrahlung photons recorded. Cu(100) and Au(100) crystals were electropolished, sputter-annealed in a preparation chamber containing low-energy electron diffraction (LEED), and transferred in vacuo into the spectrometer with a working pressure in the 10^{-11} -Torr range.

Figure 2 shows spectra at $k^{\parallel} = 0$ for Cu(100)- 1×1 and Au(100)- 5×20 . Bulk states extend up to about 2 eV above the Fermi level where a break in the curves indicates the location of the uppermost bulk states (i.e., the X'_4 point). In the gap above X'_4 a well resolved peak is seen at 0.6 eV below the vacuum level¹⁸ for both surfaces which we assign to the $n = 1$ member of a Rydberg series of image-potential states. The width of these peaks [0.3 eV full width at half maximum (FWHM)] is very close to our resolution limit. The work-function difference of 0.6 eV between the two surfaces allows us to show that the surface states are referenced to the vacuum level (and not to E_F or X'_4 or other points of the band structure). Therefore, these surface states do not represent a material-specific property (like all occupied surface states observed in photoemission) but rather the universal nature of the image potential. The Au(100)- 5×20 surface provides a further clue in this direction because it has a surface geometry totally different from the 1×1 surface, consisting of a rippled (111) layer in near registry with the (100) substrate. Further work searching for possible small effects of the surface geometry on the $n = 1$ image-potential state is in

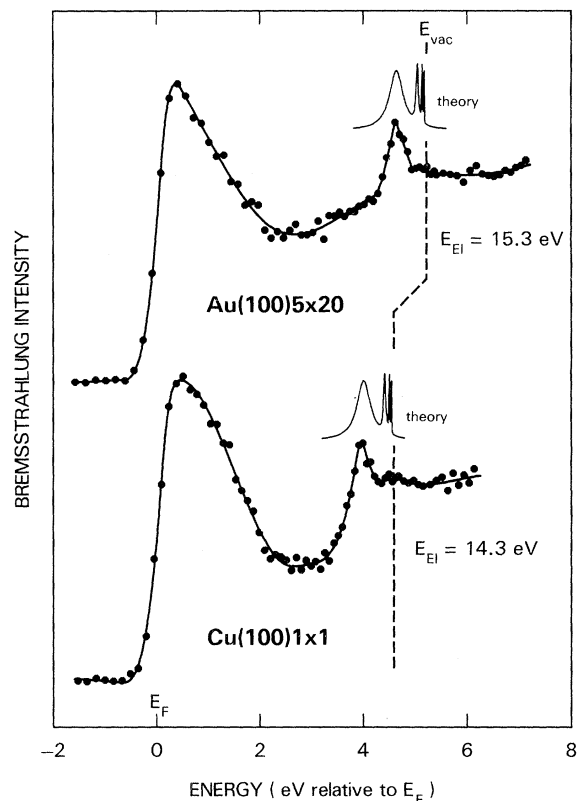


FIG. 2. Bremsstrahlung spectra for electrons incident normal to the surface ($k^{\parallel} = 0$). Sharp peaks at 0.6 eV below the vacuum level are assigned to the $n = 1$ image-potential state. The theory curves were constructed with use of the positions and widths calculated by Echenique and Pendry (Ref. 9).

progress.

Our observations match theoretical predictions of these states quite well. The curves above the data in Fig. 2 represent the calculation positions and widths of the $n = 1$ to $n = 5$ Rydberg states from Ref. 9. The $n = 1$ state is well separated from the rest of the series and from the continuum states. The latter are bunched up in a weak structure observed around E_{vac} . The calculated position of the $n = 1$ state (0.58 eV below E_{vac}) agrees with the observed values (0.64 eV for Cu and 0.63 eV for Au) within the accuracy of the measurement which is limited by the work-function determination.¹⁸ The calculated width (0.32 eV FWHM) is very close to the observed width (0.3 eV FWHM) but subtracting out the instrumental resolution suggests that these states could be substantially narrower. This, again, shows that the surface states are decoupled from the crystal wave functions. Otherwise, a lifetime broadening of typically 1 eV would be expect-

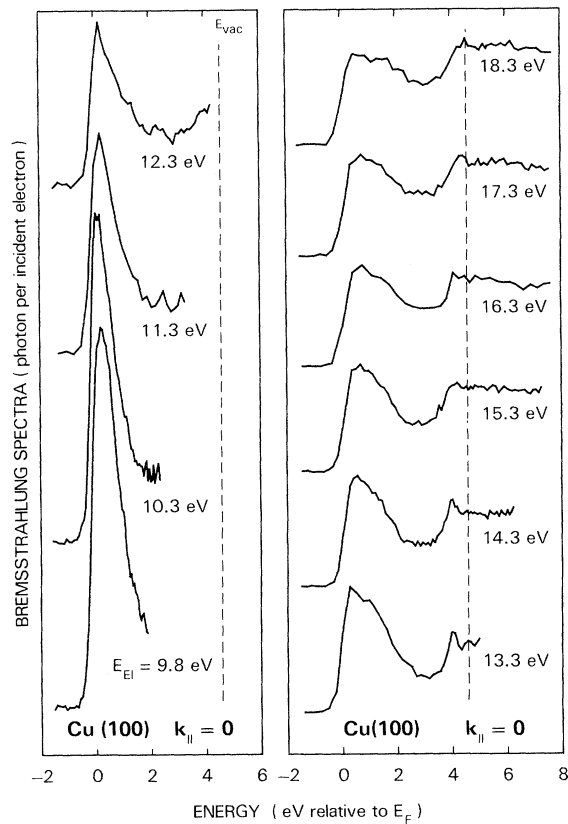


FIG. 3. Electron energy dependence of bremsstrahlung spectra at $k_{\parallel} = 0$. The image-potential state is stationary because of its two-dimensional character. Three-dimensional bulk states disperse upwards through E_F at low electron energies.

ed due to electron-hole pair creation.¹⁹ The calculation⁹ shows that the widths of higher Rydberg states decrease such that many more states might be resolved given improved instrumentation.

Figure 3 demonstrates the two-dimensional character of the surface states. By tuning the energy of the incident electrons, we change the momentum perpendicular to the surface (k^{\perp}). This should not affect the position of a two-dimensional state as long as k_{\parallel} is fixed. Indeed, we observe no change except for a broadening at higher electron energies due to decreasing resolution for the photons. Bulk states are strongly affected by a change of the electron energy. For Cu(100) and $k_{\parallel} = 0$ we are sampling bulk states along the $\Gamma\Delta X$ line in \bar{k} space (for the energy bands of Cu see Ref. 19). At electron energies less than 10.5 eV above E_F , direct interband transitions become possible from the $\Delta_1 X_1$

band down to the $\Delta_1 X'_4$ band. These can be seen as a dramatic enhancement in the intensity of the bulk states. These states are much broader (1–2 eV FWHM) than the observed surface state as a result of combined initial- and final-state lifetime broadening (compare Ref. 19). Therefore, we can rule out the alternative explanation¹⁶ of the surface state as an energy-loss replica of the bulk states.

We would like to thank Th. Fauster who set up a large portion of the experimental equipment and A. Marx, D. Grimm, and J. J. Donelon for their assistance.

¹W. Shockley, Phys. Rev. **56**, 317 (1939).

²F. J. Himpsel, Adv. Phys. **32**, 1 (1983).

³P. Heimann, H. Miosga, and H. Neddermeyer, Phys. Rev. Lett. **42**, 801 (1979).

⁴G. V. Hansson and S. A. Flodström, Phys. Rev. B **18**, 1572 (1978).

⁵H. J. Levinson, E. W. Plummer, and P. J. Feibelman, Phys. Rev. Lett. **43**, 452 (1979).

⁶S. D. Kevan, Phys. Rev. Lett. **50** 526 (1983).

⁷M. W. Cole and M. H. Cohen, Phys. Rev. Lett. **23**, 1238 (1969).

⁸J. Rundgren, and G. Malmström, Phys. Rev. Lett. **38**, 836 (1977).

⁹P. M. Echenique and J. B. Pendry, J. Phys. C **11**, 2065 (1978).

¹⁰E. G. McRae, Rev. Mod. Phys. **51**, 541 (1979).

¹¹A. Adnot and J. D. Carrette, Phys. Rev. Lett. **38**, 1084 (1977).

¹²R. F. Willis, B. Feuerbacher, and N. Christensen, Phys. Rev. Lett. **38**, 1087 (1977).

¹³R. E. Dietz, E. G. McRae, and R. L. Campbell, Phys. Rev. Lett. **45**, 1280 (1980).

¹⁴J. C. LeBosse, J. Lopez, C. Gaubert, Y. Gauthier, and R. Baudoing, J. Phys. C **15**, 3425 (1982).

¹⁵F. J. Himpsel and Th. Fauster, to be published; many design features of the new apparatus are similar to the setup described by Th. Fauster, F. J. Himpsel, J. J. Donelon, and A. Marx, Rev. Sci. Instrum. **54**, 68 (1983).

¹⁶P. D. Johnson and N. V. Smith, Phys. Rev. B **27**, 2527 (1983).

¹⁷W. Altmann, V. Dose, A. Goldmann, U. Kolac, and J. Rogozik, Phys. Rev. B **29**, 3015 (1984).

¹⁸For E_{vac} we used the work functions $\phi = 5.22 \pm 0.04$ eV for Au(100) from Ref. 4 and $\phi = 4.59 \pm 0.03$ eV for Cu(100) from P. O. Gartland, S. Berge, and B. J. Slagsvold, Phys. Norv. **7**, 39 (1973). Other published values are $\phi = 5.47$ eV for Au(100) and $\phi = 4.58$ eV, 4.76 eV, 4.8 eV, 5.10 ± 0.05 eV for Cu(100).

¹⁹J. A. Knapp, F. J. Himpsel, and D. E. Eastman, Phys. Rev. B **19**, 4952 (1979).